



Contents lists available at ScienceDirect

Journal of King Saud University – Science

journal homepage: www.sciencedirect.com

Original article

High performance of pyrochlore like $\text{Sm}_2\text{Ti}_2\text{O}_7$ heterojunction photocatalyst for efficient degradation of rhodamine-B dye with waste water under visible light irradiationK. Kaviyarasu^{a,b,*}, C. Maria Magdalane^c, D. Jayakumar^c, Y. Samson^d, A.K.H. Bashir^{a,b}, M. Maaza^{a,b}, Douglas Letsholathebe^e, Ahmed Hossam Mahmoud^f, J. Kennedy^{a,g}^a UNESCO-UNISA Africa Chair in Nanoscience's/Nanotechnology Laboratories, College of Graduate Studies, University of South Africa (UNISA), Muckleneuk Ridge, P O Box 392, Pretoria, South Africa^b Nanosciences African Network (NANOAFNET), Materials Research Group (MRG), iThemba LABS-National Research Foundation (NRF), 1 Old Faure Road, 7129, P O Box722, Somerset West, Western Cape Province, South Africa^c Department of Chemistry, St. Xavier's College (Autonomous), Tirunelveli 627002, Tamil Nadu, India^d Department of Physics, Annai Velankanni College, Tholayavattam 629157, Kanyakumari, Tamil Nadu, India^e Department of Physics, University of Botswana, Private Bag 0022, Gaborone, Botswana^f Department of Zoology, College of Science, King Saud University, Riyadh, Saudi Arabia^g National Isotope Centre, GNS Science, PO Box 31312, Lower Hutt 5010, New Zealand

ARTICLE INFO

Article history:

Received 27 September 2019

Revised 26 November 2019

Accepted 3 December 2019

Available online 16 December 2019

Keywords:

 $\text{Sm}_2\text{Ti}_2\text{O}_7$ nanosphere

Optical properties

Electron spectroscopy

Rhodamine-B dye

Photocatalytic activity

ABSTRACT

Binary metal oxide heterojunctions possibly will exclude the recombination of photogenerated charge carriers via interfacial charge transfer in assessment among the single-component photocatalytic material. Highly ordered samarium doped titania nanosphere have paid more attention to the exclusion of toxic organic pollutants. Tuning the shape, size, morphology, bandgap and defect optimization of titanium oxides ($\text{Sm}_2\text{Ti}_2\text{O}_7$) improved as an enhanced catalyst which was synthesized by using the capping agent also acts as a reducing agent. Herein, we examine an environmentally pleasant $\text{Sm}_2\text{Ti}_2\text{O}_7$ nanosphere with its various properties via assorted characterization techniques and wrapping of nanosphere makes them appropriate catalysts for the degradation of toxic dyes and show the highest efficiency via irradiation of visible light by declining the option of the exciton-recombination process. Therefore, the photocatalyst was found to produce reactive oxygen species (ROS) both in the presence and absence of light, which is responsible for the decomposition of dyes into small fractions. In addition, HRTEM study reveals that the nanospheres are highly porous nature with high active surface area and small grain size are reported in detail.

© 2019 The Author(s). Published by Elsevier B.V. on behalf of King Saud University. This is an open access article under the CC BY-NC-ND license (<http://creativecommons.org/licenses/by-nc-nd/4.0/>).

1. Introduction

Toxic organic dyes with highly complex structures play an elemental function in textile industries (Maria Magdalane et al., 2017). During the past few years, specifically industries like textile,

* Corresponding author at: UNESCO-UNISA Africa Chair in Nanoscience's/Nanotechnology Laboratories, College of Graduate Studies, University of South Africa (UNISA), Muckleneuk Ridge, P O Box 392, Pretoria, South Africa.

E-mail address: kaviyarasuloyolacollege@gmail.com (K. Kaviyarasu).

Peer review under responsibility of King Saud University.



leather, printing inks, paints, rubber, art and craft, paper, plastics, drug and cosmetics, food, utilize verity of synthetic organic dyes and pigments for the colouring purposes (Chen et al., 2010). Among all industries, the major quantity of dyes is released from the textile industries and pollute the water nearly 17–20% observed by the world bank (Amanulla et al., 2018). All these dyes are highly carcinogenic and toxic to the environment, which leads to major damages to the living organisms (Miao et al., 2018). Degradation of dyes is quite difficult by common methods like coagulation-flocculation, filtration, precipitation, solvent extraction, electrochemical treatment, ion exchange and adsorption due to the complicated chemical structure and more thermal stability of the dye effluent (Maria Magdalane et al., 2017). Titania (TiO_2) is a glowing and significant *n*-type semiconductor metal oxide for the degradation of organic dye effluent due to its towering

stability (Binas et al., 2018). Pure titania has the minimum quantum efficiency and the wider bandgap of TiO₂ confines its catalytic applications on the illumination of various light sources (Maria Magdalane et al., 2017). Recently, researches followed advanced oxidation processes (AOPs) which are ozonisation, Fenton, TiO₂ photocatalysis, photo-Fenton and photolysis using H₂O₂, etc (Manjunath et al., 2018). Among all the type of catalyst, AOPs with TiO₂ (anatase), becomes a most frequently used important semiconductor photocatalyst on irradiation of UV light source for the detoxification of pollutants (Magdalane et al., 2016). Also, a least amount percentage of light sources were used by the catalyst which leads to incomplete degradation of dyes in the industrial wastewater (Koivisto et al., 2018). Hence, all the catalysts have been to modify for the development of high-quality catalysts like metal oxide/metal oxide, metal/TiO₂, chalcogenides, etc in order to use the wide spectrum of visible light (IyyappaRajan et al., 2017). In the current literature work, the transition metal oxide and rare earth metal oxide doped titania has been carried out to stabilize the bandgap acting a major task in the photocatalytic properties of titania on the illumination of visible light (Maria Magdalane et al., 2018). The rare earth metal doped titania is developed in recent times and shows the enhanced rate of degradation efficiency on risky organic chemicals in the wastewater (Deilynazar et al., 2015).

In current research, many works have been committed for upgrading the photocatalytic activities of TiO₂, like depositing non-metal ions or noble metals (Nakamura et al., 2016). Commonly, the doping of other foreign ions is capable for the configuration of a new energy level in between the high energy conduction band and low energy valence bands of titania (Magdalane et al., 2018). Besides of titania nanostructures, A₂B₂O₇ pyrochlore is have great attention among the researches due to its multifunctional nature like radiation damage resistance, more ionic conductivity, Li-ion battery, ferroelectricity, photoluminescence, superconductivity, laser materials, fuel cells and geometrically perturbed magnetism (Reddy et al., 2018). Most of these nanostructures have high-temperature piezoelectric property, since it has high curie points and superior thermal stability like Bi₂Ti₂O₇, La₂Ti₂O₇, Nd₂Ti₂O₇, Pr₂Ti₂O₇, Ln₂Zr₂O₇ (Wang et al., 2011). Furthermore, the defects in the structure, intrinsic carrier effects and disorder on oxygen diffusion on ionic conductivity in pyrochlores. The DFT calculations of various pyrochlore structure of rare earth metal oxide was investigated apparently (Hector and Wiggan, 2004).

Many new technologies have been utilised to achieve active Sm₂Ti₂O₇ pyrochlore nanostructure, like hydrothermal processing (Lelievre and Marchet, 2017), co precipitation, sol-gel method and solution combustion method. In general, among all the methods the sol-gel method is a dominant approach to fabricate inorganic materials in recent times. In the above method, a solid precursor is hydrolysed to form a colloidal sol solution. On further reaction process the new bonds were formed along with the sol particles, these results in an immeasurable network of gel particles which yield the active nanomaterials on heating. The important advantages of this method over the other conventional method are high-purity materials and homogeneous crystalline structures can be prepared even at low temperatures. In our present work, we report the samarium doped TiO₂ with a great deal of significance due to its exceptional electrons in the *f* and *d* orbital structures. Herein we synthesis samarium doped TiO₂ by the biopolymer-mediated method and effectively applied as the competent catalyst for the degradation of dye under visible-light illumination. The rare earth metal oxide doped titania increase the distinctive UV absorption capability, high electrical conductivity, stability and huge oxygen storage space aptitude of samarium which appreciably improve the photocatalytic efficiency of TiO₂.

2. Experimental work

2.1. Synthesis of Sm₂Ti₂O₇ nanospheres

Titanium isopropoxide [Ti(OCH)(CH₃)₂]₄, Samarium nitrate [Sm(NO₃)₃·H₂O], ethanol were purchased from Sigma-Aldrich (E-Merck 99.99%) and utilised as analytical grade without any further purification. Sm₂Ti₂O₇ nanosphere was synthesised by using starch as a chelating agent. In the synthesis process, 5 g of starch was dissolved in 50 mL of pure water in the hot condition. 0.1 M Titanium isopropoxide (TIP) was prepared by using ethanol as solvent and 0.11 M samarium nitrate [Sm(NO₃)₃·H₂O] solution was prepared with double deionised water. From the above solution, 2:1 ratio Titanium isopropoxide and samarium nitrate was mixed with constant stirring. To this mixture, the solution of starch was added with continuous stirring for 2 h at 60 °C. The resulting transparent sol was cooled and boiled again in water bath at 80 °C to form a gel. The obtained gel was heated at 150 °C in a hot air oven for 10 h to get a solid. Finally, the sponge like solid was obtained which was ground in the motor and pestle to get a fine powder and this powder sample was calcinated at 600 °C for 10 h in the high temperature box furnace. The obtained solid sample was cooled, and the impurity removed by using ethanol and dried out in the oven 80 °C. The schematic representation for the synthesis of Sm₂Ti₂O₇-nanosphere as shown in Fig. 1.

3. Results and discussion

3.1. Crystalline structural determination for Sm₂Ti₂O₇

The crystalline phases of Sm₂Ti₂O₇ nanosphere were investigated via powder XRD as shown in the Fig. 2. The crystallization of Sm₂Ti₂O₇ nanosphere depends on its calcination's temperature. Samarium doped Titania calcined at 600 °C was found to be pyrochlore structure with *Fd*_{3m} crystal lattice. The intensities of the diffraction peaks in accordance with (JCPDS No.73-1699) becomes more at this calcination temperature. Furthermore, the homogenous pyrochlore structure of the sample were observed at this calcinations temperature without any other phases transformations and impurities in the samples. The crystallite size of Sm₂-Ti₂O₇ nanosphere was calculated from the Scherrer formula for the samples. The pyrochlore Sm₂Ti₂O₇ samples crystallite sizes were found to be 23 nm for the samples calcined at 600 °C (Angel Ezhilarasi et al., 2018).

3.2. Optical properties of Sm₂Ti₂O₇

The optical properties of Sm₂Ti₂O₇ nanosphere were examined by UV-vis absorption spectrum as shown in the Fig. 3. The maximum absorption peaks appear at 404 and 478 nm, the shift in the absorption peak towards red shift is due to the formation of smaller size of Sm₂Ti₂O₇ nanosphere when compared to the bulk titania $E_g = 3.2$ eV (Valsalam et al., 2019). The appearance of red shift is due to quantum size effect and confinement effects size. The bandgap of the Sm₂Ti₂O₇ nanosphere were found to be 2.6 eV (Gao et al., 2016). The bandgap of the Sm₂Ti₂O₇ nanosphere was reduced due to its calcination's temperature. The reduction in the bandgap provides the samples to absorption of higher energy photons from the visible light.

3.3. Microstructure analysis of Sm₂Ti₂O₇

The morphological analysis of Sm₂Ti₂O₇ was investigated by HRTEM images at different magnifications. The porous structures of Sm₂Ti₂O₇ nanosphere have large specific surface area at all

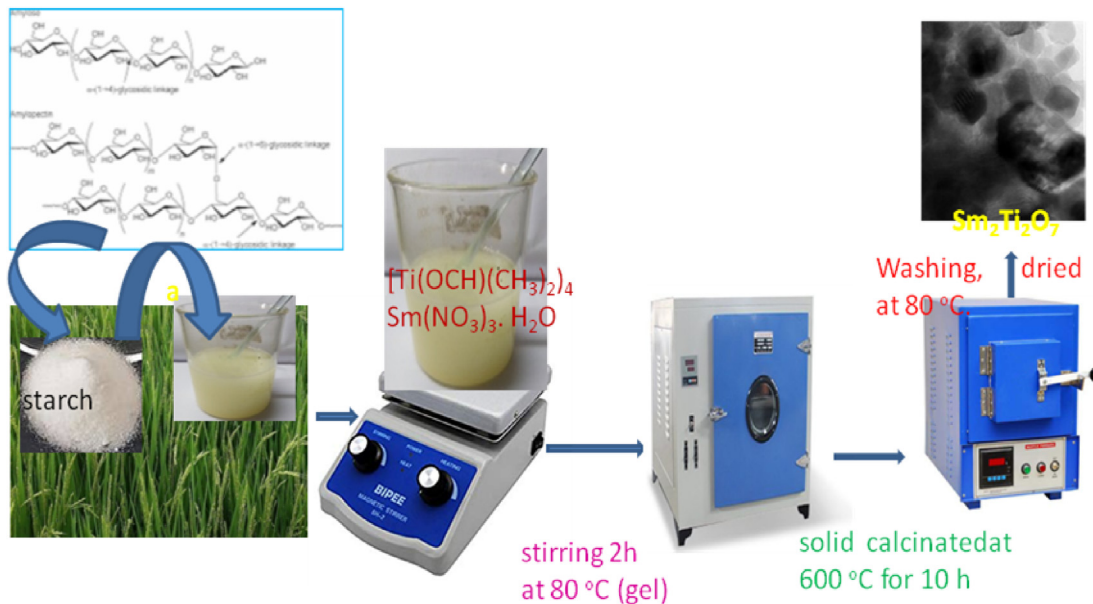


Fig. 1. Schematic representation for the synthesis of $\text{Sm}_2\text{Ti}_2\text{O}_7$ nanosphere.

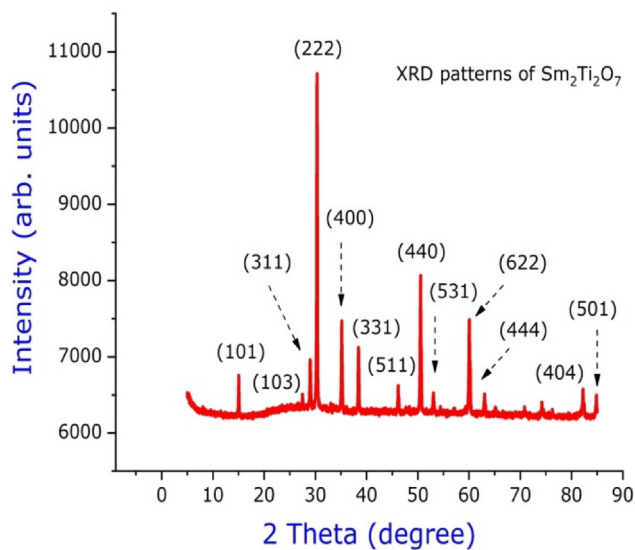


Fig. 2. XRD of $\text{Sm}_2\text{Ti}_2\text{O}_7$ nanosphere annealed at 600 °C.

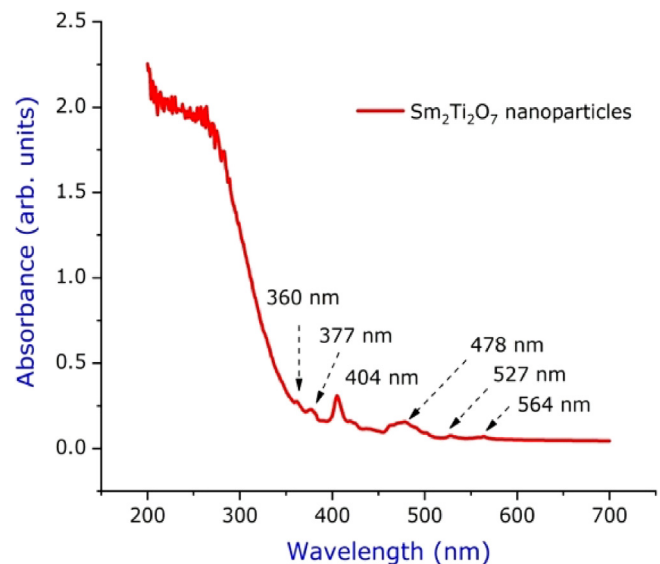


Fig. 3. UV spectrum of $\text{Sm}_2\text{Ti}_2\text{O}_7$ nanosphere annealed at 600 °C.

magnifications (Nanamats et al., 1974). The images of HRTEM appeared as an agglomerated and not exactly spherical and the average grain size is about 12 nm, which agrees with results of XRD analysis, while the morphology of oxide provided using FESEM and the results emphasize agreement with HRTEM about the agglomeration of particles as shown in Fig. 4(a-l). The samples were additional deeply magnified, and this proved an agglomerated spherical nanosphere-like morphology (Ning et al., 2010). This type of interrelated sphere-shaped porous nanostructure provides distinctive pores with a more specific active surface area. Such a crystalline structure must afford as an enhanced catalytic property (Gao et al., 2012). The morphology of nanosphere described that it may be used for recovering catalytic performance for high energy storage application (Anand et al., 2017). As evident from the literature, the size, shape and dimensions of nanostructures determines the various properties of the samples (Shao et al., 2012). As a result, by modification of the size, morphology and optical proper-

ties of the nanomaterials, the catalytic nature and selectivity can be extensively improved (Rabanal et al., 1999). The SAED pattern of $\text{Sm}_2\text{Ti}_2\text{O}_7$ nanosphere proves the polycrystalline nature of the nanostructure (Magdalane et al., 2019).

3.4. Photocatalytic activity tests $\text{Sm}_2\text{Ti}_2\text{O}_7$

The photocatalytic decomposition of industrial pollutant like synthetic RhB dye was investigated using synthesised $\text{Sm}_2\text{Ti}_2\text{O}_7$ nanosphere on irradiation of visible light. The decomposition efficiency of the synthesised samples was carried out and the absorption spectra of the resulted solution with $\text{Sm}_2\text{Ti}_2\text{O}_7$ nanosphere and blank were plotted with time (min) on illumination of visible light shown in the Fig. 5(a-c) (Nadjia et al., 2018). The synthetic RhB dye shows the absorption peaks at 498 nm with the colour change from red to colourless, which proves the decomposition of dye. The ratios between the initial concentration (C_0) and the

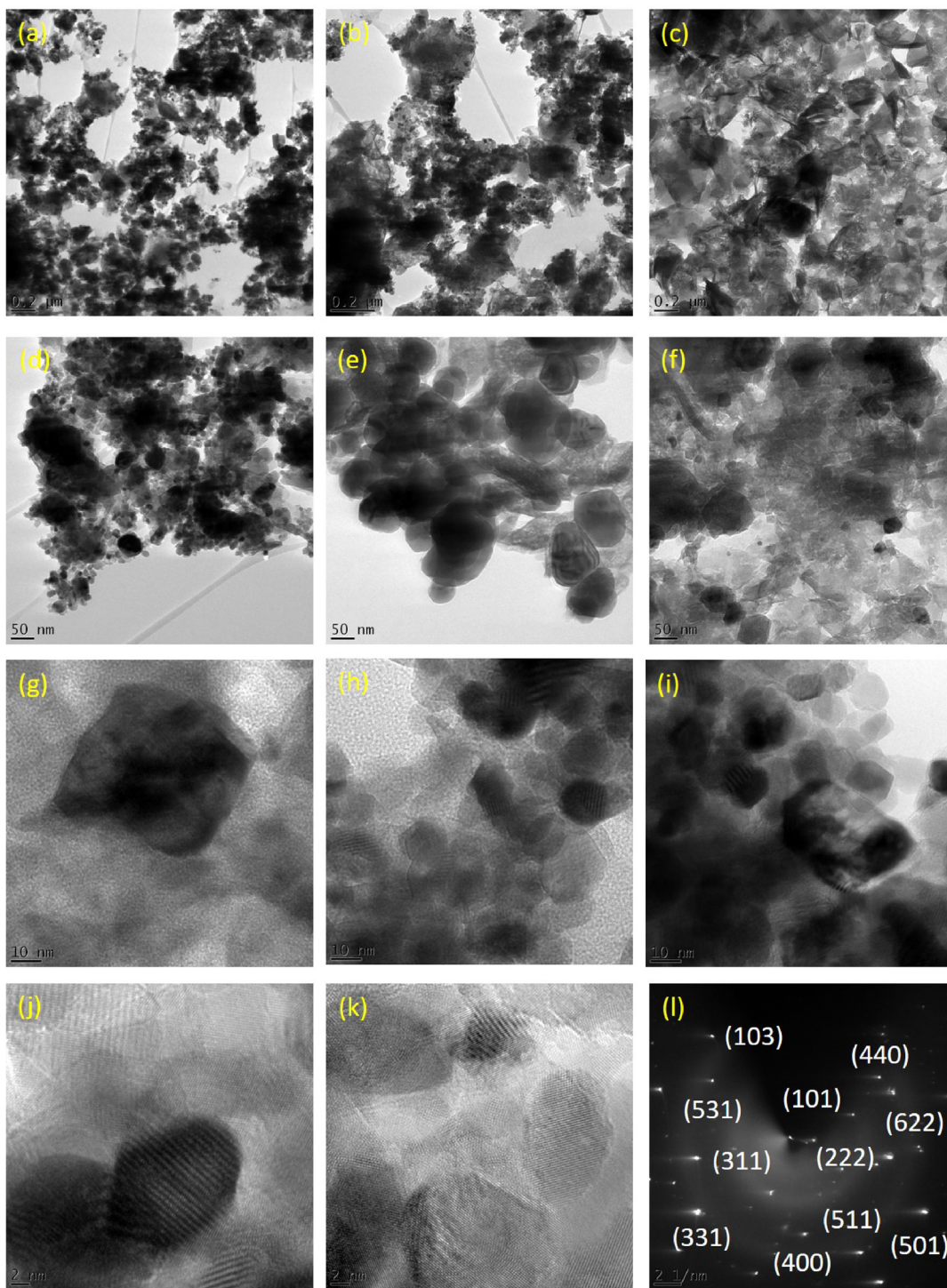


Fig. 4. (a-l) HRTEM images of $\text{Sm}_2\text{Ti}_2\text{O}_7$ nanosphere annealed at 600 °C.

concentration at time (C) of the dye (C/C_0) plotted vs time, to evaluate the effectiveness of the degradation in diverse condition (Kaviyarasu et al., 2017). The degradation efficiency of the synthesised samples found to be 94% is shown in the Fig. 5(c). The photodecomposition competence is superior for $\text{Sm}_2\text{Ti}_2\text{O}_7$ nanosphere sample. This photocatalytic experiment with the catalyst has better effect due to the more active surface area, advanced capability in the direction of absorption of visible light, lesser size effect with prominent diffusion. These extraordinary qualities of the $\text{Sm}_2\text{Ti}_2\text{O}_7$ nanosphere typically direct to an enhanced the photodegradation efficiently.

3.5. Mechanism of decomposition of RhB via $\text{Sm}_2\text{Ti}_2\text{O}_7$ nanosphere

The reaction mechanism involved in the degradation process of RhB dye with a photocatalyst via irradiation of visible light discussed in detail; Excitons are created on the surface of the photocatalyst as shown in Fig. 6. The mixture of dye solution and photocatalyst is expose via excess of visible light, the partition of electron hole can be ascribed, when the electron from valence band is absorbs photons with high energy ($h\nu > E_g$) and gets excited to conduction band.

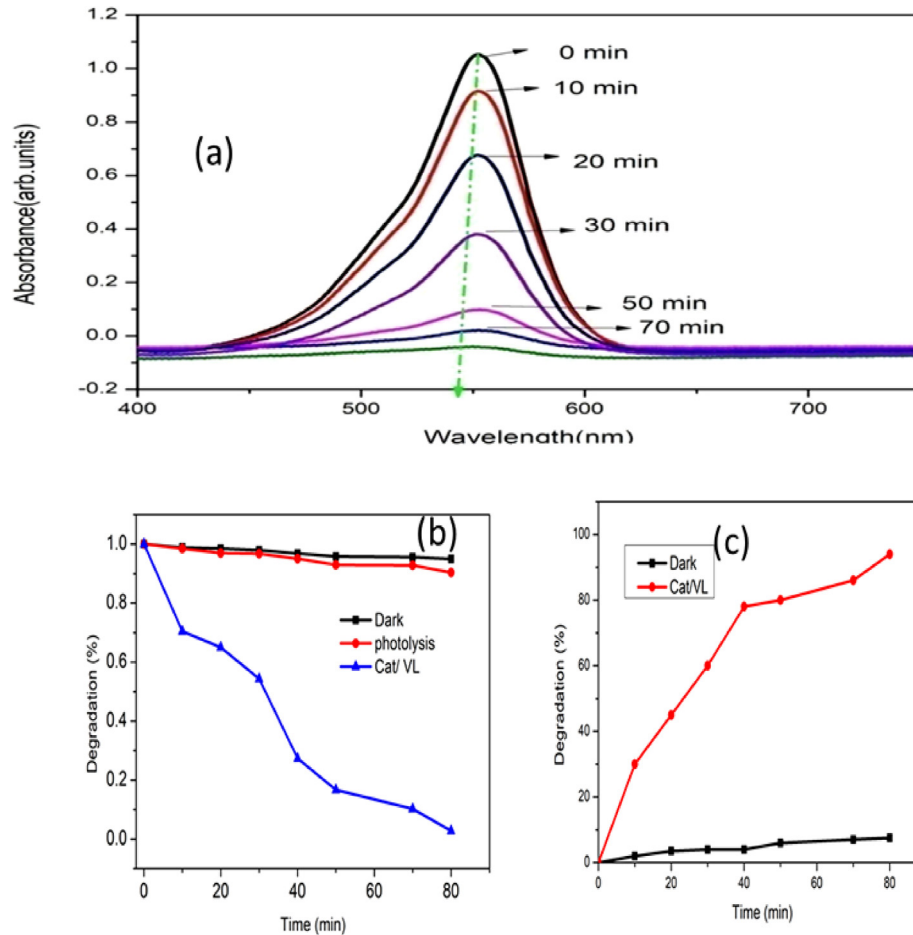
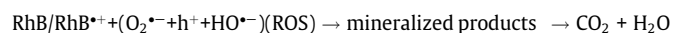
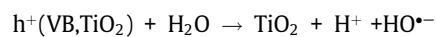
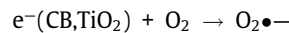
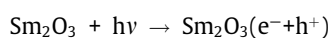
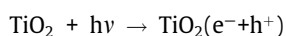
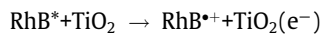
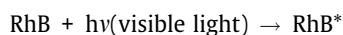


Fig. 5. (a) UV-vis absorption spectra of RhB, (dye concentration 5 mg/L, pH 9/40 mg Cat, 80 min for the reaction completion) (b) C/C_0 vs irradiation time (c) degradation % vs irradiation time.

The proposed mechanism in the decomposition reaction is a generation of photogenerated holes and electrons during the illumination of light in the mixture solution. The photogenerated holes oxidise the surface hydroxyl ions to its corresponding hydroxyl radicals (OH^\cdot) and the photogenerated electrons takes the surface oxygen molecule produce superoxide radical ($\text{O}_2^{\cdot-}$), which is again reduced to hydroperoxyl radical followed by highly oxidising agent hydrogen peroxide and finally hydroxyl radicals (OH^\cdot). In the photocatalytic reaction the organic pollutant RhB dye initially adsorbed on the catalytic surface and simultaneously it adsorbed the reactive oxygen species. During the reaction process successive intermediates are oxidized in numerous steps until mineralization to inorganic acids, water and carbon dioxide by the oxidizing species generated in the process. Many literature works reported that the unadulterated metal oxides nanoparticles show the way to quicker recombination of excitation pairs, leads to minimise the degradation of toxic dyes were as binary metal oxides drawn out the recombination process and superior relocation effectiveness of e^+ /holes, ensuing enrichment photodegradation of toxic organic dyes.



4. Conclusion

Samarium doped Titania were successfully developed by biopolymer - mediated method for deterioration of Rhodamine-B dye from the polluted waste water. $\text{Sm}_2\text{Ti}_2\text{O}_7$ nanosphere were analysed by a different characterisation analysis to describe their various properties like active surface morphology, size and optical activity. The XRD reveals that the synthesised $\text{Sm}_2\text{Ti}_2\text{O}_7$ nanospheres have the high purity and smaller grain size with good crystallinity. The degradation of Rhodamine-B dye was carried out at different parameters and photocatalytic efficiency was observed nearly 94% owing to the smaller grain size, high active surface area, and better absorption of light source with prominent diffusion of dyes. These extraordinary qualities of the samples typically direct to an enhanced photodegradation efficiently. Interestingly, prepared nanostructures revealed the promising growth inhibition of bacteria. The mutual effect of excitons pair recombination, crystallinity and active surface area accountable for the superior photocatalytic and antibacterial activity.

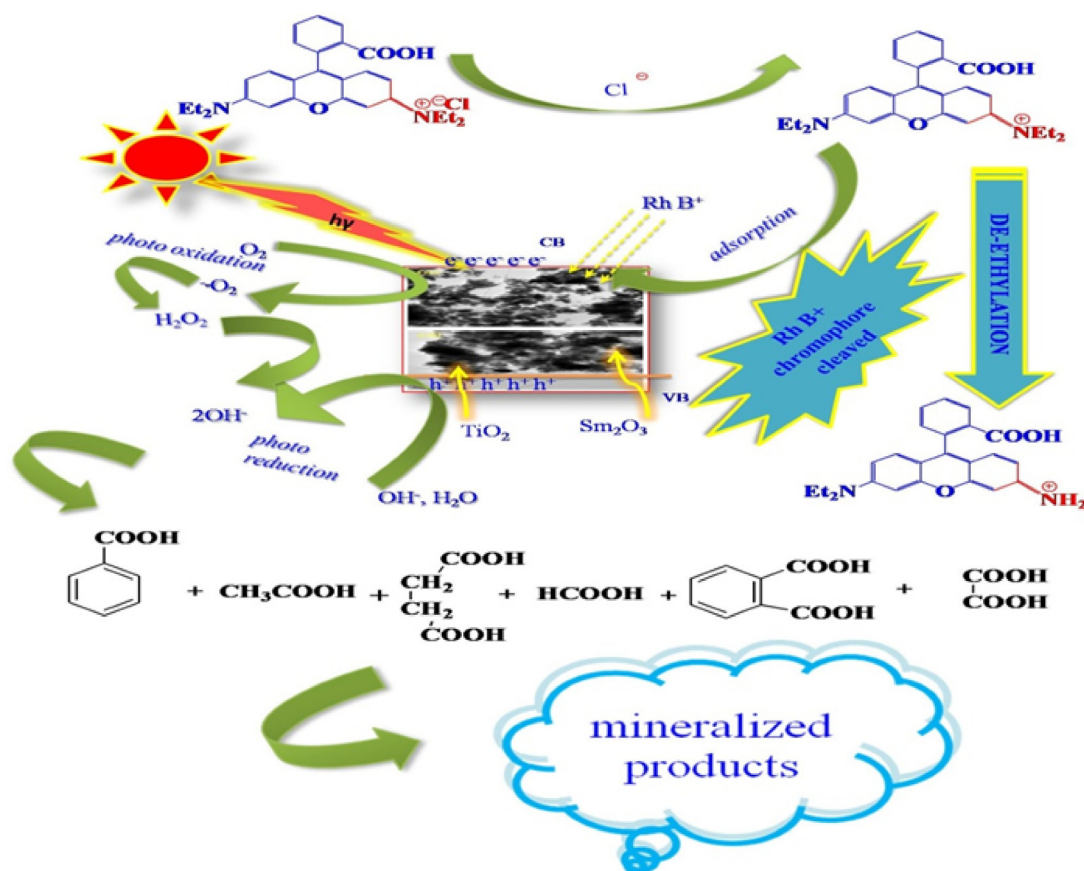


Fig. 6. General mechanism in degradation process of RhB dye with a photocatalyst via irradiation of visible light.

Declaration of Competing Interest

The authors declare that they have no known competing financial interests or personal relationships that could have appeared to influence the work reported in this paper.

Acknowledgment

The authors extend their appreciation to The Researchers supporting project number (RSP-2019/108) King Saud University, Riyadh, Saudi Arabia.

References

- Amanulla, A.M., Shahina, S.K., Sundaram, R., Magdalane, C.M., Kaviyarasu, K., Letsholathebe, D., Mohamed, S.B., Kennedy, J., Maaza, M., 2018. Antibacterial, magnetic, optical and humidity sensor studies of β -CoMoO₄ - Co₃O₄ nanocomposites and its synthesis and characterization. *J. Photochem. Photobiol. B: Biology*.
- Anand, K., Kaviyarasu, K., Muniyasamy, S., Mohana Roopan, S., Gengan, R.M., Chuturgoon, A.A., 2017. Bio-synthesis of silver nanoparticles using agroforestry residue and their catalytic degradation for sustainable waste management. *J. Cluster Sci.* 28, 2279–2291.
- Angel, Ezhilarasi A., Judith Vijaya, J., Kaviyarasu, K., John Kennedy, L., Jothi Ramalingam, R., Al-Lohedan, Hamad A., 2018. Green, synthesis of NiO nanoparticles using Aegle marmelos leaf extract for the evaluation of in-vitro cytotoxicity, antibacterial and photocatalytic properties. *J. Photochem. Photobiol. B: Biology*.
- Binas, V., Papadaki, D., Maggos, Th., Katsanaki, A., Kiriakidis, G., 2018. Study of innovative photocatalytic cement - based coatings: the effect of supporting materials. *Constr. Build. Mater.* 168, 923–930.
- Chen, X., Shen, S., Guo, L., Mao, S.S., 2010. Semiconductor-based Photocatalytic Hydrogen Generation. *Chem. Rev.* 110, 6503–6570.
- Deilynazar, N., Khorasani, E., Alaein, M., Hashemifar, S.J., 2015. First-principles insight sint of magnetism: a case study on some magnetic pyrochlores. *J. Magn. Mater.* 393, 127–131.
- Gao, Z., Wu, L., Lu, C., Gu, W., Zhang, T., Liu, G., Xie, Q., Li, M., 2016. The anisotropic conductivity of ferroelectric La₂Ti₂O₇-ceramics. *J. Eur. Ceram. Soc.* 89, 121–135.
- Gao, Z.P., Yan, H.X., Ning, H.P., Reece, M.J., 2012. Ferroelectricity of Pr₂Ti₂O₇ ceramics with super-high curie point. *Adv. Appl. Ceram.* 112, 69–74.
- Hector, A.L., Wiggin, S.B., 2004. Synthesis and structural study of stoichiometric Bi₂Ti₂O₇ pyrochlore. *J. Solid State Chem.* 177, 139–145.
- IyyappaRajan, P., Judith Vijaya, J., Jesudoss, S.K., Kaviyarasu, K., John Kennedy, L., Jothiramalingam, R., Al-Lohedan, Hamad A., 2017. Mansoor-Ali Vaali-Mohammed, Green-fuel-mediated synthesis of self-assembled NiO nano-sticks for dual applications - photocatalytic activity on Rose Bengal dye and antimicrobial action on bacterial strains. *Mater. Res. Express* 4, (8) 085030.
- Kaviyarasu, K., Kanimozhi, K., Matinise, N., Maria Magdalane, C., Mola, Gene T., Kennedy, J., Maaza, M., 2017. Antiproliferative effects on human lung cell lines A549 activity of cadmium selenide nanoparticles extracted from cytotoxic effects: investigation of bio-electronic application. *Mater. Sci. Eng., C* 76, 1012–1025.
- Koivisto, A.J., Jensen, A.C., Kling, K.I., Kling, J., Budtz, H.C., Koponen, I.K., Tuinman, I., Hussein, T., Jensen, K.A., Norgaard, A., Levin, M., 2018. Particle emission rates during electrostatic spray deposition of TiO₂ nanoparticle-based photoactive coating. *J. Hazard. Mater.* 341, 218–227.
- Lelievre, J., Marchet, P., 2017. Structure and properties of Bi₂Ti₂O₇ pyrochlore-type phase stabilized by lithium. *J. Alloys Compd.* 45, 45–51.
- Magdalane, C.M., Kanimozhi, K., Arularasu, M.V., Ramalingam, G., Kaviyarasu, K., 2019. Self-cleaning mechanism of synthesized SnO₂/TiO₂ nanostructure for photocatalytic activity application for waste water treatment. *Surf. Interfaces* 17, 100346.
- Magdalane, C.M., Kaviyarasu, K., Vijaya, J.J., Siddhardha, B., Jeyaraj, B., 2016. Photocatalytic activity of binary metal oxide nanocomposites of CeO₂/CdO nanospheres: investigation of optical and antimicrobial activity. *J. Photochem. Photobiol., B* 163, 77–86.
- Magdalane, C.M., Kaviyarasu, K., Matinise, N., Mayedwa, N., Mongwaketsi, N., Letsholathebe, D., Mola, G.T., AbdullahAl-Dhabi, N., ValanArasu, M., Henini, M., Kennedy, J., Maaza, M., Jeyaraj, B., 2018. Evaluation on La₂O₃ garlanded ceria heterostructured binary metal oxide nanoplates for UV/ Visible light induced removal of organic dye from urban wastewater. *S. Afr. J. Chem. Eng.* 26, 49–60.
- Manjunath, K., Reddy Yadav, L.S., Jayalakshmi, T., Reddy, V., Rajanaika, H., Nagaraju, G., 2018. Ionic liquid assisted hydrothermal synthesis of TiO₂ nanoparticles: photocatalytic and antibacterial activity. *J. Mater. Res. Technol.* 7 (1), 7–13.
- Maria, Magdalane C., Kaviyarasu, K., Raja, A., Arularasu, M.V., Mola, Gene T., Isaev, Abdulgalim B., Al-Dhabi, Naif Abdullah, MariadhasValanArasu, B., Jeyaraj, J., Kennedy, M. Maaza, 2018. Photocatalytic decomposition effect of erbium doped cerium oxide nanostructures driven by visible light irradiation: Investigation of

- cytotoxicity, antibacterial growth inhibition using catalyst. *J. Photochem. Photobiol.*, B 185, 275–282.
- Maria, Magdalane C., Kaviyarasu, K., Judith Vijaya, J., Siddhardha, B., Jeyaraj, B., Kennedy, J., Maaza, M., 2017a. Evaluation on the heterostructured $\text{CeO}_2/\text{Y}_2\text{O}_3$ binary metal oxide nanocomposites for UV/Vis light induced photocatalytic degradation of Rhodamine-B dye for textile engineering applications. *J. Alloys Compd.* 727, 1324–1337.
- Maria, Magdalane C., Kaviyarasu, K., Judith Vijaya, J., Siddhardha, B., Jeyaraj, B., 2017b. Facile synthesis of heterostructured cerium oxide/yttrium oxide nanocomposite in UV light induced photocatalytic degradation and catalytic reduction: Synergistic effect of antimicrobial studies. *J. Photochem. Photobiol.*, B 173, 23–34.
- Maria, Magdalane C., Kaviyarasu, K., Judith Vijaya, J., Jayakumar, C., Maaza, M., Jeyaraj, B., 2017c. Photocatalytic degradation effect of malachite green and catalytic hydrogenation by UV-illuminated CeO_2/CdO multilayered nanoplatelet arrays: Investigation of antifungal and antimicrobial activities. *J. Photochem. Photobiol.*, B 169, 110–123.
- Miao, J., Zhang, R., Zhang, L., 2018. Photocatalytic degradations of three dyes with different chemical structures using ball-milled TiO_2 . *Mater. Res. Bull.* 97, 109–114.
- Nadjia, L., Abdalkader, E., Naceur, B., Ahmed, B., 2018. CeO_2 nanoscale particles: Synthesis, characterization and photocatalytic activity under UVA light irradiation. *J. Rare Earths.* 87, 1–13.
- Nakamura, K., Mori, M., Itoh, T., Ohnuma, T., 2016. Theoretical and experimental investigation of defect formation / migration in $\text{Gd}_2\text{Ti}_2\text{O}_7$: General rule of oxide-ion migration in $\text{A}_2\text{B}_2\text{O}_7$ pyrochlore. *AIP Advances* 6, 115003.
- Nanamats, S., Kimura, M., Doi, K., Matsushi, S., Yamada, N., 1974. New ferroelectric $\text{La}_2\text{Ti}_2\text{O}_7$. *Ferroelectrics* 8, 511–519.
- Ning, H.P., Yan, H.X., Reece, M.J., 2010. Piezoelectric strontium niobate and calciumniobate ceramics with super – high curie points. *J. Am. Ceram. Soc.* 93, 1409–1413.
- Rabanal, M.E., Vaarez, A., Amador, U., ArroyoDompablo, E., GarcoaAlvarado, F., 1999. Structure and reaction with lithium of tetragonal pyrochlore-like compound $\text{Sm}_2\text{Ti}_2\text{O}_7$. *J. Mater. Process. Technol.* 92, 529–533.
- Reddy, Y.S., Magdalane, C.M., Kaviyarasu, K., Mola, G.T., Kennedy, J., Maaza, M., 2018. Equilibrium and kinetic studies of the adsorption of acid blue 9 and Safranin O from aqueous solutions by MgO decorated FLG coated Fuller's earth. *J. Phys. Chem. Solids* 123, 43–51.
- Shao, Z., Saitzek, S., Roussel, P., Ferri, A., Mentre, O., Desfeux, R., 2012. Investigation of microstructure in ferroelectric lead-free $\text{La}_2\text{Ti}_2\text{O}_7$ thin film grown on (001) SrTiO_3 substrate. *Cryst. Eng. Comm.* 14, 6524–6533.
- Valsalam, S., Agastian, P., ValanArasu, M., Al-Dhabi, N.A., Ghilan, A.K.M., Kaviyarasu, K., Ravindran, B., Chang, S.W., Arokiyaraj, S., 2019. Rapid biosynthesis and characterization of silver nanoparticles from the leaf extract of *Tropaeolummajus* L. and its enhanced in-vitro antibacterial, antifungal, antioxidant and anticancer properties. *J. Photochem. Photobiol.*, B 191, 65–74.
- Wang, J., Zhang, F., Lian, J., Becker, U., 2011. Energetics and concentration of defects in $\text{Gd}_2\text{Ti}_2\text{O}_7$ and $\text{Gd}_2\text{Zr}_2\text{O}_7$ pyrochlore at high pressure. *Acta Mater.* 59, 1607–1618.